Macromolecules **2006,** *39,* 9435−9440

Sol−Gel Transition of Hydrophobically Modified Polyrotaxane

Takeshi Karino,[†,§] Yasushi Okumura,[‡,§] Changming Zhao,[‡] Masatoshi Kidowaki,[‡,§]
Toshiyuki Kataoka,[†] Kohzo Ito,[‡,§] and Mitsuhiro Shibayama*,[†,§]

Neutron Science Laboratory, Institute for Solid State Physics, University of Tokyo,
Tokai, Ibaraki, 319-1106, Japan, Graduate School of Frontier Sciences, University of Tokyo, Kashiwa,
Chiba 277-8561, Japan, and CREST, Japan Science and Technology Agency, 4-1-8 Honcho Kawaguchi
Saitama, 332-0012 Japan

Received September 22, 2006; Revised Manuscript Received November 3, 2006

ABSTRACT: The sol−gel transition and thermosensitivity of methylated polyrotaxane (Me−PR) aqueous solutions were investigated by means of small-angle neutron scattering (SANS) and dynamic light scattering (DLS). It is known that water-solubility of polyrotaxane (PR), consisting of poly(ethylene glycol) (PEG) and α-cyclodextrin (α-CD), is very low due to stacking of neighboring α-CD molecules on a PEG chain. Methylation of the hydroxyl groups on α-CD molecules resulted in a significant improvement of water-solubility, and Me−PR exhibited a thermoreversible sol−gel transition in water depending on the degree of methylation. For low degrees of methylation (≤30%), a Me−PR solution was transparent even up to 80 °C. On the other hand, for high degrees of methylation (≥60%), it became opaque with increasing temperature and a gelation took place at high temperature. The temperature dependence of the sliding motion of α-CD molecules along the PEG chains and the mechanism of sol−gel transition are discussed on the basis of SANS and DLS results.

1. Introduction

Polyrotaxanes (PRs) are a class of supramolecules which consisit of linear polymer chains and ring molecules threaded by the polymer chains. One typical PR is made of poly(ethylene glycol) (PEG) and α-cyclodextrin (α-CD).[1,2] α-CD is a cyclic oligosaccharide having 18-hydroxyl groups on the surface and is an amphiphilic molecule with hydrophilic outside and hydrophobic inside. α-CD molecules are spontaneously threaded by a PEG chain in water due to hydrophobic interactions between the PEG chain and the inner part of the α-CD molecule. Because of the unique architecture of PRs, many researchers have studied PRs not only theoretically and experimentally, but also for applications in industrial, medical, pharmaceutical, cosmetic fields, and so on.

Okumura et al. developed a new type of gel called “slide-ring gel” (SR gel) having “movable” cross-links.[3] SR gels consist of PR chains of which α-CDs are cross-linked to each other. The SR gel has novel physical properties: (1) Spatial inhomogeneities decrease with increasing cross-link concentrations at low cross-link concentrations.[4] (2) Under uniaxial deformation, a two-dimensional small-angle neutron scattering (SANS) pattern shows a normal butterfly pattern, indicating that deformation of polymer chains in the gel is similar to those of the polymer solution.[5] This pattern is the first observation for polymer gel. These results suggest that movable cross-links allow PR chains in a SR gel to behave like linear polymer chains in a solution. (3) As a matter of fact, Zhao observed a decay mode in SR gels, exclusively appearing between the so-called gel mode (ascribed to permanent or transient networks) and the translational mode of individual polymer chains.[6]

However, there are only a few kinds of solvents which dissolve PRs. This is due to the molecular structure of α-CD. α-CD molecules have a tendency to self-aggregate via hydrogen bonding of their hydroxyl groups on the outer surface of α-CD. Bonini et al. investigated β-cyclodextrin molecules in water by means of dynamic light scattering (DLS) and cryo-transmission electron microscopy.[7] They reported that β-cyclodextrin molecules form large aggregates even in low concentrations. As a result, PRs becomes insoluble in many kinds of solvent. Dimethyl sulfoxide (DMSO) and strong alkali aqueous solutions are some of the few exceptions which dissolve PRs. Recently, Araki et al. reported that PRs are also soluble in dimethylacetamide/lithium chloride.[8] However, the solubility of PRs is still very low for various solvents. This low solubility of PRs has been restricting the applicability of PRs for industrial use.

Recently, we succeeded in preparation of water-soluble polyrotaxanes by introducing hydrophobic groups.[9,10] In the case of methyl group substitution, i.e., methylated polyrotaxane (Me−PR), Me−PR aqueous solutions exhibited thermosensitivity and underwent a sol−gel transition by increasing temperature. Figure 1 is a schematic illustration showing (a) polyrotaxane and (b) methylated polyrotaxane. Because of the substitution, hydrogen bonding between α-CD rings is strongly suppressed. On the other hand, introduction of methyl groups to PRs leads to thermosensitivity as will be extensively discussed in this paper. It is noted here that substitution with larger hydrophobic functional groups, such as ethyl groups and propyl groups, resulted in a macrophase separation even at ambient temperature. It was rather surprising that Me−PR was very soluble in water.

In this paper, we discussed the thermosensitivity and sol−gel transition of Me−PRs having different degrees of methylation and the effects of methylation on the structure by SANS and DLS.

2. Experimental Section

2.1. Preparation of Me−PR. Polyrotaxane was prepared with poly(ethylene glycol) (PEG) and α-cyclodextrin (α-CD). PEG was purchased from Fluka, Co. Ltd. and its weight-average molecular weight, M_w, was 3.5×10^4. The filling ratio (FR) of α-CD, i.e., the number of α-CD molecules per polyrotaxane was estimated at

---

* To whom correspondence should be addressed. E-mail: shibayama@issp.u-tokyo.ac.jp.
[†] Neutron Science Laboratory, Institute for Solid State Physics, University of Tokyo.
[‡] Graduate School of Frontier Sciences, University of Tokyo.
[§] CREST, Japan Science and Technology Agency.

10.1021/ma062203z CCC: $33.50

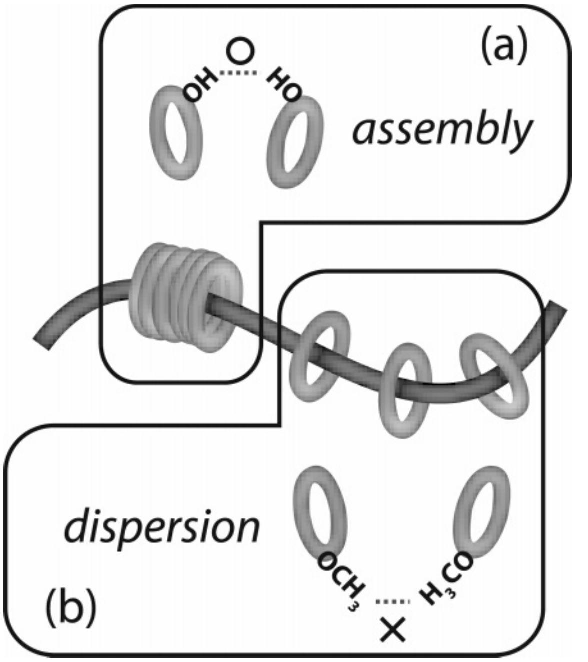

Figure 1. Schematic model of (a) hydrogen bonding of polyrotaxane molecules via α-CD rings and (b) methylated polyrotaxane, Me−PR, which has a low capability of hydrogen bonding.

ca. 110 by ^{1}H−NMR. This corresponds to that 27% of a PEG chain is covered with α-CDs (an α-CD molecule covers two PEG monomer units.). The hydroxyl groups on each α-CD molecule were substituted by methyl groups using sodium hydride and iodomethane. The details of sample preparation are described elsewhere.[9] The methylation was controlled by the amount of iodomethane and sodium hydride with respect to the OH groups of polyrotaxane.

The degree of methylation, f_m, is defined by f_m = (the number of methyl groups per glucose unit)/3 × 100 %. The degree of methylation was estimated from ^{1}H−NMR spectra by comparing the integration of the OH and ^{1}H signals of α-CD with that of other protons. Thus, five kinds of Me−PRs were prepared having different f_ms, i.e., M20 ($f_m = 20\%$), M30 ($f_m = 30\%$), M60 ($f_m = 60\%$), M80 ($f_m = 80\%$), and M100 ($f_m = 100\%$).

2.2. Small-Angle Neutron Scattering (SANS). SANS experiments were carried out at the SANS-U spectrometer, Institute for Solid State Physics, University of Tokyo, Tokai, Japan.[11] The two-dimensional detector (64 × 64 cm ^{2}) was placed at either 2 or 8 m from the sample. The incident neutron wavelength was 7.0 Å. The temperature was varied from 20 to 80 °C. The observed scattering intensity functions, $I(q)$, were corrected for air scattering, incoherent scattering, and transmission and then were rescaled to the absolute intensity, with a polyethylene secondary standard, where q is the magnitude of the scattering vector. The Me−PR samples were soluble in deuterated water. The polymer concentration was 0.1 g/mL.

2.3. Dynamic Light Scattering (DLS). DLS experiments were carried out on a static/dynamic compact goniometer (SLS/DLS-5000), ALV, Langen, Germany. A He−Ne laser with 22 mW (wavelength $\lambda = 632.8$ nm) was used as the incident beam at a fixed angle of 90°. Time−intensity correlation functions, $g^{(2)}(\tau)$, were measured for Me−PR aqueous solutions as a function of temperature from 20 to 80 °C. The heating and cooling rate is 0.45 K/min. The polymer concentration was 0.05 g/mL. The solutions were filtered with 0.45 μm Millpore filter. The obtained $g^{(2)}(\tau)$s were analyzed with CONTIN, a constrained regularization method for inverting data represented by linear algebraic or integral equations,[12] in order to obtain the decay rate distribution function, $G(\Gamma^{-1})$.

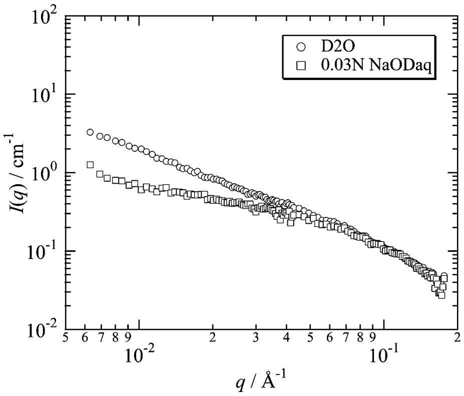

Figure 2. SANS intensity functions, $I(q)$s, of M20 in D_2O and in 0.03 N NaOD.

3. Results and Discussion

3.1. Effect of Methylation. As discussed in the Introduction, PRs are not soluble in water. On the other hand, methylated polyrotaxane (Me−PR) is soluble in water. Figure 2 shows SANS intensity functions, $I(q)$s, of M20 in D_2O and in 0.03 N NaOD aqueous solutions at 20 °C. $I(q)$ of M20 in D_2O increased in the low q-region. On the other hand, such an excess scattering was suppressed for M20 in 0.03 N NaOD. The excess scattering of M20 in D_2O indicates existence of large concentration fluctuations due to the stacking of α-CD molecules. In alkali solutions, however, excess scattering seems to be suppressed by repulsive interaction of dissociated α-CD molecules. It is clear from this figure that M20, i.e., Me−PRs having a low degree of methylation, are soluble in water. Note that $I(q)$s in the high q-region are almost identical. This indicates that the local chain conformation is the same, independent of the type of solvents. In order to obtain a microscopic picture, we analyzed the SANS data by using following equation. $I(q)$ is described with the so-called Ornstein−Zernike (OZ) function, i.e., a scattering function for semidilute polymer solution$_s$

$$I(q) = \frac{I(0)}{1 + q^2\xi^2} \tag{1}$$

where ξ is the correlation length, and $I(0)$ is the zero-scattering intensity. The observed $I(q)$s were satisfactorily fitted with eq 1. Figure 3a shows $I(q)$s for Me−PRs in D_2O at 20 °C having different f_ms. It is clear that $I(q)$s at low q regions are suppressed with increasing f_m. The dotted lines in the inset of Figure 3a shows the result of curve-fitting with the OZ function, i.e., $1/I(q)$ vs q^2 plot. Figure 3b shows the correlation length, ξ, as a function of f_m. This result indicates that α-CD rings in Me−PR are molecularly dispersed along a PEG chain owing to methylation of α-CD.

3.2. Thermosensitivity of Methylated PRs. Figure 4 shows the temperature, T, dependence of light scattered intensity, $\langle I \rangle$, for Me−PRs having different f_ms during heating (open symbols) and cooling (solid symbols) between 20 and 80 °C. The scattering angle was 90°. $\langle I \rangle$ of M30 did not change noticeably with increasing and decreasing temperature. In addition, the solution was transparent irrespective of temperature. On the other hand, $\langle I \rangle$ s of M60 and M80 exhibited strong thermosensitivity. That is, $\langle I \rangle$ drastically increased with increasing T. It should be noted that the viscosity of the solutions increased and the solutions finally became gels by increasing T close to the seep rise in $\langle I \rangle$. Both M60 and M80 became opaque at high temperatures, e.g., $T > 60$ °C. All of these phenomena indicate structural reorganization of Me−PRs depending on the differ-

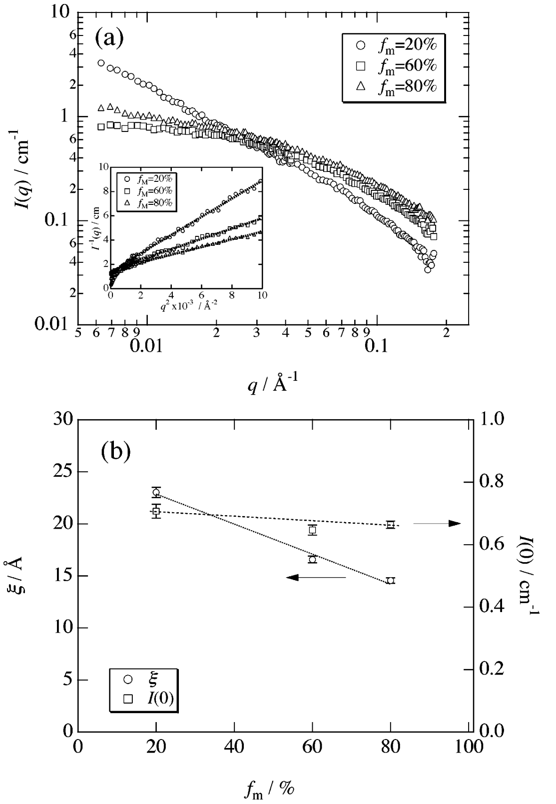

Figure 3. (a) $I(q)$s of Me−PRs in D_2O at 20 °C having different f_ms. The inset shows the Ornstein−Zernike (OZ) plots ($1/I(q)$ vs q^2). (b) f_m dependence of the correlation length, ξ .

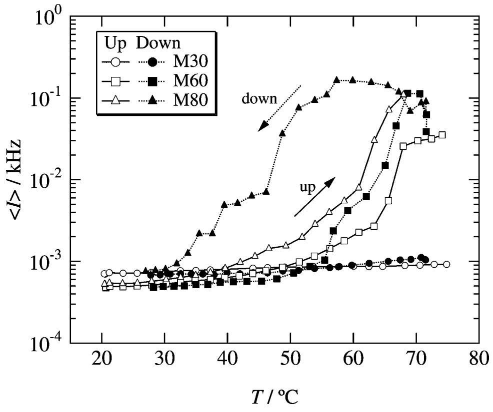

Figure 4. Light-scattering intensity, 〈I〉 as a function of temperature. Open circle is the rising process. Closed circle is the down process.

ence of hydrophobicity of polyrotaxane, i.e., f_m. It is also noteworthy that 〈I〉 of M80 shows a large hysteresis during T-scans. 〈I〉 for M80 started to increase at $T \simeq 50$ °C up to 70 °C. On the other hand, 〈I〉 in the cooling process has a plateau at high value until $T \simeq 50$ °C, and then steeply decreases to a similar value before heating. It is conjectured that α-CD molecules are dispersed at low temperatures, but they start to aggregate by increasing T due to hydrophobic interaction between methyl groups on CD molecules. This tendency is controlled by the degree of methylation. This is why the temperature variation of 〈I〉 has a strong f_m dependence. The presence of hysteresis in the 〈I〉−T curve is due to formation of large clusters which require a long time relaxation.

3.3. The Structure in Solution. Figure 5 shows the temperature dependence of SANS intensity functions, $I(q)$s, for M30. The inset shows the OZ plots. $I(q)$s were independent of temperature. As shown in Figure 4, Me−PRs having low f_ms did not show thermosensitivity. Hence, the SANS results are consistent with the LS results.

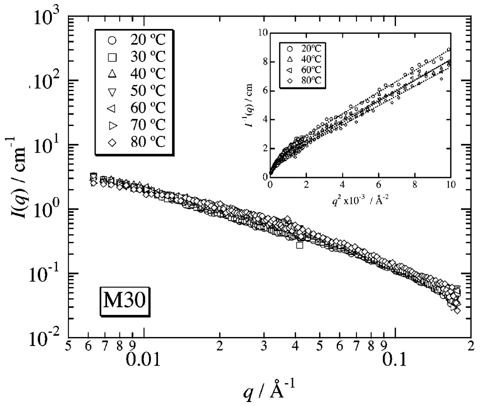

Figure 5. $I(q)$ s for M30 measured at various temperatures. The inset shows the OZ plots. No temperature dependence was observed.

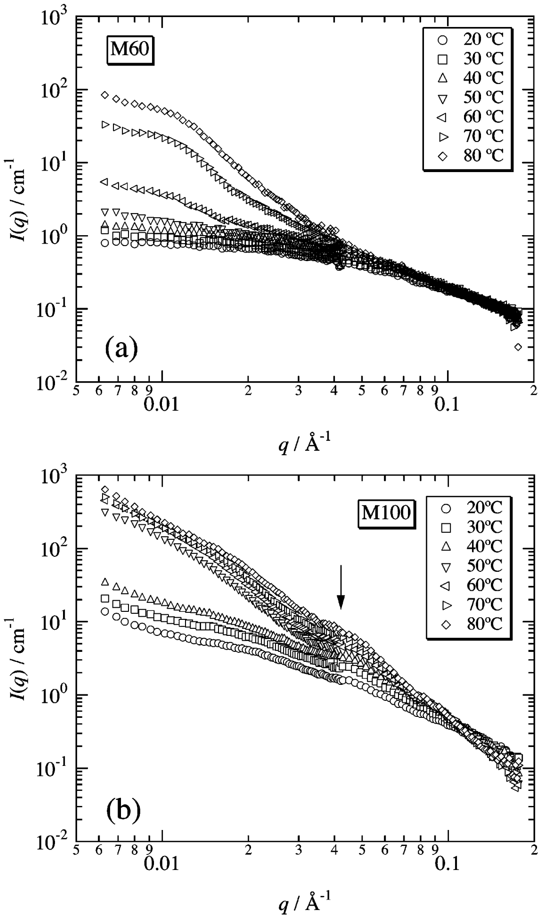

Figure 6. Temperature dependence of $I(q)$s for (a) M60 and (b) M100.

Figure 6 shows the temperature dependence of $I(q)$s for (a) M60 and (b) M100. In contrast to the results of M30, $I(q)$ drastically changed in the high-temperature region, i.e., $T > 60$ °C. At low temperatures, $I(q)$s were monotonic decreasing functions. With increasing temperature, $I(q)$ of M60 increased gradually, and drastically changed at the sol−gel transition temperature (≃ 60°C). These $I(q)$ variations are similar to those of a sol−gel transition of block copolymer solutions.[13,14] In the gel state, $I(q)$ had a characteristic shoulder about $q = 0.015$ Å^{-1} . In M100, by increasing the temperature, hydrophobic interactions between methylated α-CD molecules become dominant, resulting in formation of hydrophobic domains with

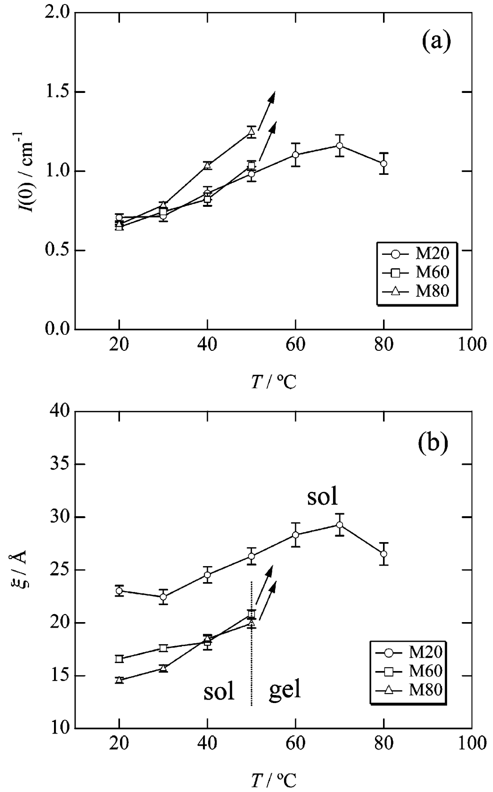

Figure 7. Temperature dependence of $I(0)$ and ξ for M20, M60, and M80. The arrows indicate divergence of $I(0)$ and ξ above this temperature due to gelation.

clustered α-CD molecules. As a result, a shoulder appears in $I(q)$s as indicated with an arrow.

Figure 7 shows temperature variations of (a) $I(0)$ and (b) the correlation length, ξ, for M20, M60, and M80, evaluated with eq 1. Both $I(0)$ and ξ increase with T. This is due to an increase in the hydrophobic interaction between the methyl groups on α-CD and water, and the concentration fluctuations increase with T. For Me−PRs with higher f_ms, i.e., M60 and M80, ξ values are much lower than those of M20, suggesting a finer dispersion of α-CD in M60 and M80 than in M20. That is, by substituting methyl group, CD molecules are dispersed molecularly on the PEG chain.

3.4. The Microstructure in the Gel State. Above the gelation temperature, on the other hand, the scattering pattern shows not only the rapid increase of intensity but also a characteristic shoulder. Figure 8a shows the so-called Kratky plots (i.e., $q^2I(q)$ vs q) of M60 and M80 above gelation temperatures. In the gel state, the plots show a single peak. In order to elucidate the gel structure, we calculated the characteristic size of the gel state using following equation,

$$I(q) = I(0)\exp\left(-\frac{R_G{}^2q^2}{3}\right) \qquad (2)$$

where R_G is the radius of gyration and $I(0)$ is the zero-scattering intensity. In this case, R_G means the size of the hydrophobic domains. This scattering function means that the gel structure was composed of both CD domains and polymer chains. The appearance of a peak in a Kratky plot indicates the presence of a gel phase. This indicated that the system was gel phase. This result was similar to the sol−gel transition of poly(vinyl alcohol).[15]

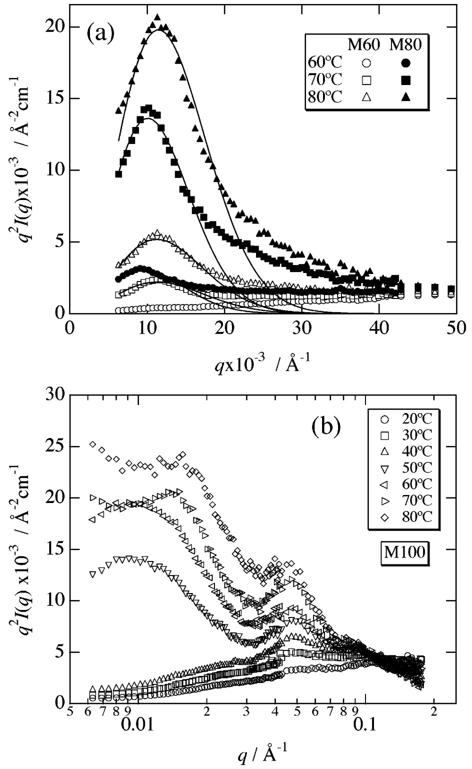

Figure 8. Kratky plots of M100 at various temperatures. Several scattering peaks are clearly resolved.

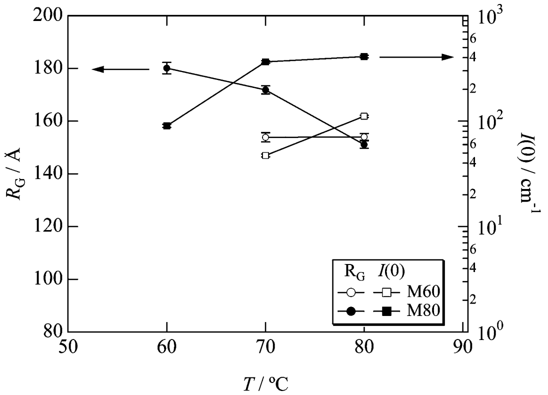

Figure 9. Temperature dependence of R_G and $I(0)$ for M60 and M80.

Figure 8b shows the Kratky plots of M100. It is clear that there are several peaks in the curves for $T \geq 60$ °C. The peaks around 0.015 Å^{-1} $\lesssim q \lesssim$ 0.03 Å^{-1} seem to have the same origin as those discussed above, i.e., the spatial inhomogeneities exclusively appearing in gel state. On the other hand, those at $q \approx 0.05$ Å^{-1} and at $q \approx 0.08$ Å^{-1} may indicate a formation of microphase separated structure. The ratio of the q values of these peaks is 1: $\sqrt{3}$, suggesting either hexagonal packing of cylindrical domains or body-centered-cubic packing of spherical domains ($\sqrt{2}$ being missing due to smearing effect of SANS). These microdomains might be formed by aggregation of methylated α-CD molecules due to strong hydrophobic interactions. However, it is an open question why an ordered structure with a Bragg spacing of $2\pi/q \approx 126$Å^{-1} is observed.

Figure 9 shows the temperature dependence of R_G for M60 and M80 above the transition temperature. The zero-q scattering intensity of M80 was larger than that of M60. This may indicate that the high methylated polyrotaxane was strongly aggregated between hydrophobically CD molecules, resulting in increase of scattering intensity at elevated temperatures. R_G of M80 decreases with increasing T, indicating that collapsing of

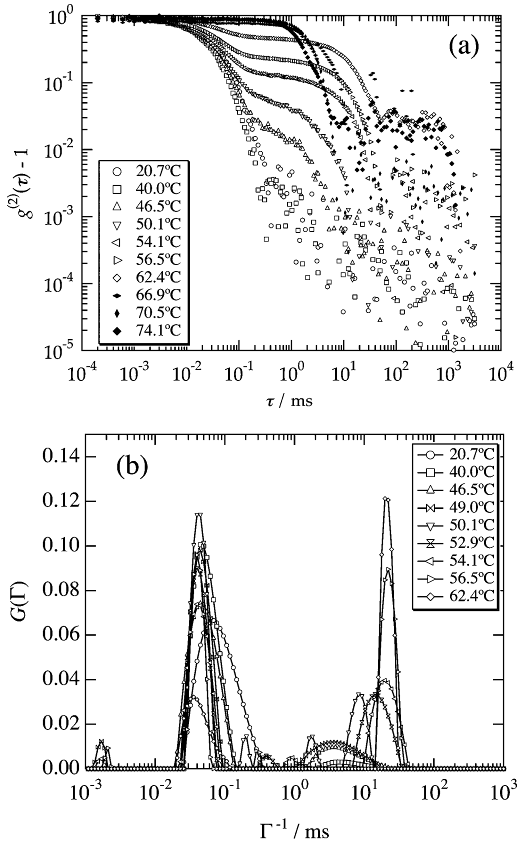

Figure 10. (a) Time−intensity correlation functions (TICF) and (b) the decay-rate distribution functions, $G(\Gamma^{-1})$, of M60 at various temperatures.

hydrophobic domains takes place. Such behavior is not observed in M60, probably due to a weaker T dependence.

3.5. Chain Dynamics. In the previous works, the sliding motion of CD molecules along the PEG chain was observed by dynamic light scattering.[6] The decay time distribution function obtained by CONTIN analysis showed three peaks. The fast mode is ascribed to the so-called collective mode observed in semidilute solutions and in gels. The slow mode was the translational mode. A middle mode between the fast and slow modes is reported to appear exclusively in slide-ring gels, i.e., in polyrotaxyane gels.

Figure 10 shows the time−intensity correlation function (TICF), $g^{(2)}(\tau) - 1$ of M60 obtained at various temperatures, where τ is the decay time. At $T \leq 40°$, the TICFs have a single decay around $\tau \approx 5 \times 10^{-1}$ ms. Above this temperature, a plateau appeared in the $10^{-1} < \tau < 10^{1}$ ms region, for which the tail becomes longer, with increasing T. Above $T \geq 50$ °C, a slow mode emerged around $\tau \approx 20$ ms. The former, i.e., the fast relaxation corresponds to the gel mode, while the latter (the slow mode) is the translational mode of Me−PR in solution. In this figure, the sliding mode reported elsewhere was not resolved.[6] This may be due to the following reason. In ref 6, the polyrotaxane was cross-linked via movable cross-links. Because of such restriction, the sliding mode could be clearly observed. On the other hand, in the case of this study, Me−PR molecules were not cross-linked and α-CD molecules move as backbone PEG chain moves. Above the gelation temperature, Me−PR became a gel and α-CD rings are aggregated via hydrophobic interaction. Thus, the sliding motion is again frozen. Apart from the sliding motion, Figure 10 clearly indicates that the sol−gel transition took place around $T \approx 50$ °C, which is in accordance with the results of Figure 4.

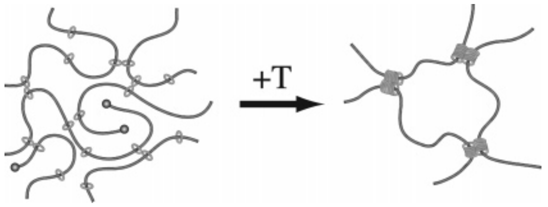

Figure 11. Schematic models showing the temperature dependence of Me−PR in solutions.

3.6. Mechanism of Sol−Gel Transition. As discussed in the previous sections, it is clear that methylation of α-CD on polyrotaxane leads to a dramatic thermosensitivity of Me−PR in aqueous solutions. There are two effects of methylation. One is an increase of solubility of PR by reducing the capability of hydrogen bonding of α-CD. The other is introduction of thermosensitivity owing to the presence of hydrophobic methyl groups on α-CD. As a result, Me−PR exhibits unique properties in aqueous solutions. Figure 11 shows the gelation mechanism of hydrophobically modified polyrotaxane. α-CD molecules are hydrophilic molecules. On the other hand, methylated CD molecules are hydrophobic molecules because of the introduction of hydrophobic methyl groups. In low f_ms, the hydrophobic domains are distributed randomly. Hence, Me−PRs did not show thermoresponsibility in the whole temperature range. In high f_m s, on the other hand, CD molecules on Me−PRs self-aggregated owing to strong hydrophobic interaction between methyl groups. These aggregation processes are in analogy to the sol−gel transition of hydrophobically modified cellulose.

4. Conclusion

The solution properties and sol−gel transition of methylated polyrotaxane (Me−PR) were investigated by means of small-angle neutron scattering and dynamic light scattering. Substitution of hydroxyl groups on α-CD rings on polyrotaxane with methyl groups led to an increase in water solubility. Without methylation, polyrotaxane chains aggregated easily due to the interaction of α-CD molecules and/or aggregates. The methyl groups prevent formation of the hydrogen-bonding network among neighboring α-CD molecules. The degree of methylation, f_m, was varied, and the solution properties were investigated as a function of f_m. At low f_m (≈30%), Me−PR became soluble in water and no thermosensitivity was observed. On the other hand, at high f_ms, such as $f_m = 60$ and 100%, marked thermosensitivity appeared and Me−PR exhibited a sol−gel transition around at 60°C. It was found that a microphase separated structure was formed and it formed a network structure. Sliding motion was observed neither in the sol state nor in the gel state. In the sol state, sliding motion is non-observable due to synchronized motion of the backbone PEG chains and α-CD rings. In the gel state, on the other hand, cross-links made of aggregated α-CD rings are frozen-in. The sol−gel transition curve with respect to T showed a marked hysteresis due to long-time relaxation of hydrophobically aggregated clusters. It is demonstrated that solubility and thermosensitivity of polyrotaxanes can be tuned by methylation of α-CD rings.

Acknowledgment. This work is supported by Core Research for Evolutional Science and Technology (CREST), Japan Science and Technology Agency, Japan. T.K. acknowledges the support by CREST. This work was partially supported by the Ministry of Education, Science, Sports and Culture, Japan (Grant-in-Aid, 18205025 and 18068004). The SANS experiment was performed with the approval of Institute for Solid-state

Physics, The University of Tokyo (Proposal No. 05-5561), at Japan Atomic Energy Agency, Tokai, Japan.

References and Notes

(1) Harada, A.; Kamachi, M. *Macromolecules* **1990**, *23*, 2821.

(2) Harada, A.; Li, J.; Kamachi, M. *Nature (London)* **1992**, *356*, 325.

(3) Okumura, Y.; Ito, K. *Adv. Mater.* **2001**, *13*, 485−487.

(4) Karino, T.; Okumura, Y.; Ito, K.; Shibayama, M. *Macromolecules* **2004**, *37*, 6117−6182.

(5) Karino, T.; Okumura, Y.; Zhao, C.; Kataoka, T.; Ito, K.; Shibayama, M. *Macromolecules* **2005**, *38*, 6161−6167.

(6) Zhao, C.; Domon, Y.; Okumura, Y.; Okabe, S.; Shibayama, M.; Ito, K. *J. Phys.: Condens. Matter* **2005**, *17*, S2841−S2846.

(7) Bonini, M.; Rossi, S.; Karlsson, G.; Almgren, M.; Lo Nostro, P.; Baglioni, P. *Langumuir* **2006**, *22*, 1478−1484.

(8) Araki, J.; Ito, K. *J. Polym. Sci. Part A: Polym. Chem.* **2006**, *44*, 532−538.

(9) Kidowaki, M.; Zhao, C.; Kataoka, T.; Ito, K. *Chem. Commun.* **2006**, 4102−4103.

(10) Kataoka, T.; Kidowaki, M.; Zhao, C.; Minamikawa, H.; Shimizu, T.; Ito, K. *J. Phys. Chem. B* **2006**, *110*, 24377−24383.

(11) Okabem, S.; Nagao, M.; Karino, T.; Watanabe, S.; Adachi, T.; Shimizu, H.; Shibayama, M. *J. Appl. Crystallogr.* **2005**, *38*, 1035−1037.

(12) Provencher, S. W. *Comput. Phys. Commun.* **1982**, *27*, 213.

(13) Okabe, S.; Sugihara, S.; Aoshima, S.; Shibayama, M. *Macromolecules* **2003**, *35*, 8139−8146.

(14) Fuse, C.; Okabe, S.; Sugihara, S.; Aoshima, S.; Shibayama, M. *Macromolecules*,**2004**, *37*, 7791−7798.

(15) Shibayama, M.; Kurokawa, H.; Nomura, S.; Muthukumar, M.; Stein, R.S.; Roy, S. *Polymer* **1992**, *33*, 2883−2890.

MA062203Z